HUNTINGTON MEDICAL RESEARCH INSTITUTES
NEUROLOGICAL RESEARCH LABORATORY
734 Fairmount Avenue
Pasadena, California 91105

Contract No. N01-NS-8-2399
Quarterly Progress Report
Oct 1-Dec 31, 1999
Report No. 5

"Microstimulation of the Lumbosacral Spinal Cord"

Douglas B. McCreery, Ph. D.
Albert S. Lossinsky, Ph.D.
Leo Bullara, B.A.
Ted G. F. Yuen, Ph.D..
William F. Agnew, Ph.D.

SUMMARY AND ABSTRACT

We have continued to develop procedures for implanting our form-fitting microelectrode array into the feline sacral spinal cord. In this array, 6 discrete activated iridium microelectrodes extend from a circular array superstructure 3 mm in diameter. The underside of the superstructure is contoured into a saddle-shaped concavity, which straddles the convex dorsal surface of the sacral spinal cord. The arrays are implanted using a high speed inserter instrument which injects the arrays into the cord a velocity of approximately 1m/sec.

During the past quarter, four arrays were implanted into the sacral cord of 4 cats. Twenty-nine to 33 days after implantation of the arrays, the cats were anesthetized with Propofol, and 2 of the 6 microelectrodes were pulsed for 12 hours on each of 2 successive days. The stimulus was cathodic-first, controlled-current pulses, 150 μs/phase in duration, delivered continuously at a rate of 20 Hz. The stimulus amplitude was 80 or 100 μA (12 or 15 nC/ph). Thus, in these animals, the stimulus frequency was lower (20 Hz) but the stimulus amplitude was greater than in previous animals. The cats were sacrificed within 30 minutes after the second day of stimulation.

The histologic analysis revealed that most of the microelectrode tips were close to their targets in the intermediolateral cell column. There was very little tissue injury along the tracks themselves. However, in most cases, healed glial scars extended ventrally from the tip sites. We believe that these were caused during implantation of the array, when the spinal cord was momentarily compressed vertically and expanded horizontally. We have subsequently altered the settings on our introducer instrument with the objective of minimizing this type of injury.

In spite of the glial scars, in most cases there was healthy neuropil and neurons adjacent to the electrode tip sites, and this allowed us to continue our investigation of the safety of various stimulation protocols. When the stimulus pulse amplitude was 80 μA (12 nC/ph), most of the neurons adjacent to the tip sites appeared to be normal although one shrunken hyperchromic cell was observed very close to one of the pulse tips. In contrast, the tips of both electrodes in cat Sp108 that were pulsed at 100 μA (15 nC/ph) were surrounded by aggregates of lymphocytes, a phenomena that we have observed only once previously in the spinal cord series. We have consistently observed these aggregates around pulsed microelectrodes in the cerebral cortex when the cats are sacrificed within 12 hours at the start of stimulation. However, the lymphocytes around the intracortical electrodes begin to disperse within approximately 48 hours, even when the stimulation is continued. We have attributed the absence of lymphocytes in the cat spinal cord to the fact that the stimulus regimens always spanned at least 36 hours. The presence of lymphocytes in cat Sp108 at 36 hours after the start of stimulation suggests that the aggregates may persist longer when the stimulus charge per phase is greater.

METHODS

In the past quarter, we implanted 3 of the bilateral microelectrode arrays into the sacral spinal cords of 3 cats (Sp106, Sp107 and Sp108). The iridium microelectrodes have active geometric surface areas of approximately 2,000 μm^2 at their tips. Six discrete activated iridium microelectrodes extend from a circular array superstructure 3 mm in diameter. The underside of the superstructure is contoured into a saddle-shaped concavity, which straddles the convex dorsal surface of the sacral spinal cord. This is intended to place their tips within the intermediolateral cell column of the S_2 sacral spinal cord when the array's concave bottom is centered over the cord's midline.

The arrays were implanted using aseptic surgical techniques, with the cats anesthetized with halothane and nitrous oxide. The scalp was opened longitudinally in a midline incision and a percutaneous connector was affixed to the skull. The electrode array and cables were tunneled subcutaneously to the sacral region, and the spinal cord was exposed from L_5 to S_3 with a standard dorsal laminectomy. The L_5 dorsal spinal process was secured with a vertebral clamp and the spinal dura was opened in a longitudinal midline incision extending from S_1 to S_3. The S_2 level of the cord was located approximately by recording the dorsal cord potential while electrically stimulating the perigenital region, which is innervated from the S_2 level of the cord. The arachnoid was then dissected from the spinal roots in the S_2 region, so the roots could be retracted. The recording electrode was inserted through a separate small opening in the dura and passed approximately 4 cm caudally, so as to lie adjacent to the ventral roots. It was then secured to the dura with one additional suture. The recording reference electrode was secured to the outside of the dura at approximately the same level as the recording electrode. Two 7-0 sutures were passed through the margins of the dura. These were later used to close the dura.

The microelectrode array was then placed into the end of the stator tube (barrel) of the inserter tool, where it is held against the armature by a vacuum. The array cable was secured loosely to the dura, approximately 2 cm rostral to the implant site. The orifice of the barrel was centered over the midline of the sacral cord, with the array cable extending rostrally. Figure 1 shows 3 frames from the intraoperative video during insertion of the electrode array into the central cord of Cat Sp108. Figure 1A shows the barrel of the inserter tool resting on the surface of the sacral cord. The instrument is mounted on the stereotaxic apparatus. The array is protected within the barrel of the insertion instrument and its upper surface is held against the sliding cylinder by a vacuum. When the trigger is released, the sliding cylinder and the array are propelled downwards by a spring. At the end of the insertion stroke (Figure 1B), a valve mechanism automatically collapses the vacuum and the array is released so that the introducer tool can be withdrawn. Figure 1C shows the array's superstructure resting on the dorsal columns of the sacral cord, with the electrodes penetrating down into the cord. After inserting the array, the margins of the dura were loosely approximated by drawing up the two 7-0 sutures. The array cable was then secured firmly to the dura. The partly open dura was covered with a patch of fascia resected from the parispinal muscles. The platinum ground electrode was placed on top of the fascia patch. The muscles were then approximated with sutures and the skin was closed with staples.

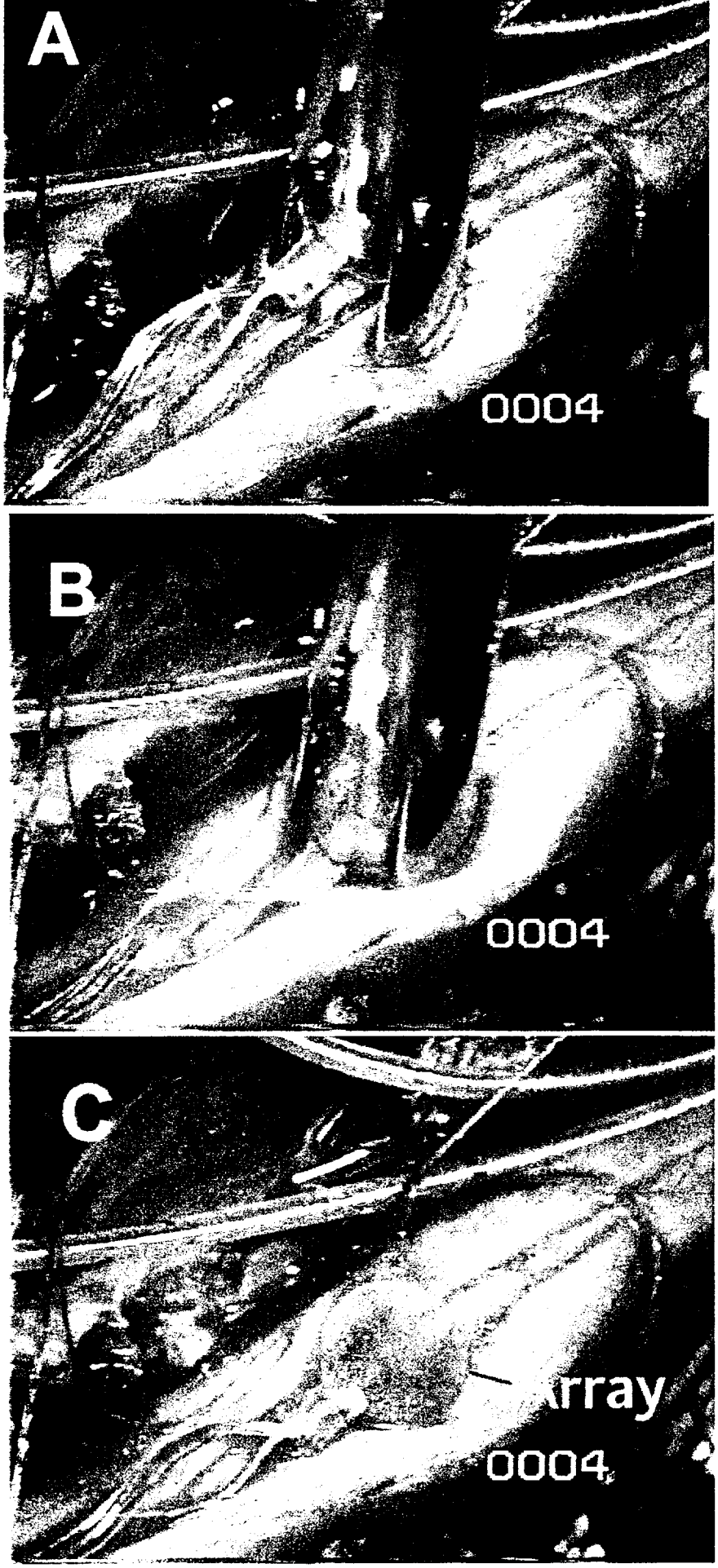

Figure 1

In the arrays implanted into cats Sp106, Sp107 and Sp108, we omitted the two long (3 mm) iridium stabilizing pins that were a feature of the original design. The pins effectively stabilized the arrays after insertion, but they damaged the cord's ventral funiculus. Without the long pins, the arrays do appear to be stable during several weeks in vivo, but the omission of the long pins does render the arrays less stable during the implant surgery. For example, in cat Sp107, we attempted to secure the electrode cable to the dura before the array had been stabilized by partially closing the dura. The array partially dislodged from the cord. Rather than re-insert the array at another location, we elected to complete the insertion at the original location by pressing down on the array superstructure with the barrel of the inserter tool. The spinal cord sustained significant injury, either while the array was being partially dislodged, or during the attempt to re-insert it in this unorthodox manner.

Twenty-nine to 33 days after the implant surgery, the 2-day stimulation regimens were initiated. The cats were anesthetized with Propofol and 2 or 3 of the 6 intraspinal microelectrodes were pulsed for 12 hours on each of two consecutive days. The stimulus waveform was cathodic-first, controlled-current pulses.

Cat/ Days post-implant	Electrode	µA	Hz	Pulse width (µs)	Charge/ph (nC)
SP106 / 29-30	1	80	20	150	12
SP106 / 29-30	6	80	20	150	12
SP107 / 37-38	1	80	20	150	12
SP107 / 37-38	2	80	20	150	12
sp107/ 37-38	4	80	20	150	12
SP108 / 33-34	1	100	20	150	15
SP108 / 33-34	2	100	20	150	15
SP108 / 33*	6*	80	20	150	12

*Electrode 6 in SP108 was pulsed for 12 hours on day 1 only, ending 24 hours before perfusion.

The compound action potentials evoked by each of the intraspinal microelectrodes were recorded via the subdural recording electrode, adjacent to the ventral roots. In most cases, the response to 1024 successive stimulus pulses was summated to obtain an averaged response. The responses were acquired before the start of the first 12 hours of stimulation, and at the end of the first and second 12-hour sessions. Responses were acquired using a graded sequence of pulse amplitudes, so that the threshold of the neuronal responses could be estimated. The responses were acquired using the same type of stimulus pulse sequence used during the subsequent 12-hour test stimulus (cathodic first pulse pair, 150 µs/phase in duration).

Immediately after the end of the second day of stimulation, the animals were deeply anesthetized with pentobarbital and perfused through the ascending aorta with a prewash solution consisting of 300-900 ml of phosphate-buffered saline, to remove blood, followed by 4 L of ½ strength Karnovsky's Fixative in 0.1 M sodium phosphate buffer at pH 7.3 (½ K). We determined that fixation of the spinal cord was improved by increasing the duration of the pre-wash phase (to 3 minutes, from the original 2 minutes), and the addition of 0.05% procaine hydrochloride to the prewash solution, in order to dilate blood vessels. The sacral spinal cord was resected and the

capsule of connective tissue covering the elongated array matrix was removed, leaving the array *in situ*. The spinal roots and nerves were identified to determine the exact level of the array.

Tissue processing. The array was removed, and the tissue blocks were indexed with a small dot of tissue-marking ink applied to their cut rostral surface. Tissue blocks were immersion-fixed overnight in the above-mentioned fixative. Because we have occasionally experienced wrinkling of the tissue during sectioning of the paraffin-embedded spinal cord, we decided to compare two methods of embedding the tissue. Method A (standard method): After fixing the spinal cord tissue blocks in our standard ½ K fixative, the blocks were dehydrated through a graded series of ethanol, gradually increasing the concentration of ethanol to 100%. Next, the tissue was cleared in HEMO-D clearing agent after which the blocks were gradually introduced into heated liquid paraffin. The tissue blocks were then embedded in 100% paraffin, sectioned at 8 µm and stained with either Nissl or hematoxylin and eosin (H & E).

Method B. Tissue blocks from the sacral or lumbar spinal cord of cat Sp107, adjacent to the blocks containing the electrode tracks, were washed overnight in PBS and then for 2 hrs in distilled water to remove aldehyde fixatives not bound to the tissue proteins. After washing, the tissues were dehydrated in a graded series of ethanol, as in Method A, and embedded into paraffin. The paraffin-embedded tissue was cut at a thickness of 6 µm and stained with Nissl or with H&E stains.

RESULTS

Histology

Overview. The electrode arrays were found to be positioned along the dorsal midline of the spinal cord, usually in S_1 or S_2 (Figure 2) and similar to Sp104 and Sp105 (Quarterly progress report # 4). Histologic evaluations of electrode tracks produced by the electrodes in these three animals revealed that some of the electrode tips were in or near their intended target, the intermediolateral cell column. Based on the spatial relationship between the electrode tip sites and the pattern of gliotic scarring in these three cats, it is likely that the electrodes at some time penetrated deeper than their intended target. The specific histologic changes are presented below. The general pattern of histologic changes associated with the electrode tips included variable gliotic scarring, neovascularization and vascular hyperplasia, as well as neuronal changes that included chromatolysis, in some cases within 200 µm of the electrode tracks and also more distant from the electrode tracks and tip sites. Neuronal changes were especially apparent in Sp107 which presented the most gliotic scarring. As noted previously, much of the injury in cat Sp107 probably occur as a result of the particular procedure employed during the implant surgery. Our surgical procedure was modified as a result of our experience with this animal.

Vasculitis, perivascular leukocytic infiltration and occasional darkened and shrunken neurons were present adjacent to the some of the electrode tips sites that had been pulsed at high amplitude, as discussed below.

Sp106.

Histologic analysis of Sp106 indicated that the tips of electrodes #1-4 (Figures 3 and 7) were in the desired target of the intermediolateral cell column, while electrodes #5 and #6 were positioned more medial to the intermediolateral cell column (Figure 9). Tissue changes included acellular gliotic scars without hemosiderin pigments. The patterns made by the gliotic scars suggested that the electrodes were directed more laterally (Figure 4) in this animal. Although one neuron very close to the tip site was shrunken and hyperchromic (Figure 5), most of the neurons associated with pulsed and unpulsed electrodes within a 200 µm radius their tips appeared normal (Figures 6, 8).

Sp107.

Sp107 presented histologic changes not observed in either Sp106 or Sp108. There was mechanical displacement of the dorsal surface of the spinal cord. Leukocytes were observed

between the undersurface of the array and the meninges. Within the cord, electrodes #1-3 were directed somewhat medially while electrodes #4-6 were directed slightly laterally (Figure 10). It appears that the array was not properly centered when we attempted to re-insert it manually after it had become partially dislodged. There was vasculitis and gliosis adjacent to the electrode tracks, indicating an unusual degree of dispersed trauma in this animal. Neuronal changes were remarkable, especially in one large focus medial to (unpulsed) electrode #6. This focus contained neurons undergoing chromatolysis, but these changes were not localized to the vicinity of the electrode tip (Figure 11). We did not observe aggregates of leukocytes surrounding the electrode tips, or surrounding any of the blood vessels near the electrode tips. Tissue obtained from the caudal portion of the sacral cord was processed with the alternative Method B. This method demonstrated improved tissue sectioning and staining (Figures 12, 13).

Sp108.

In Sp108, the tips electrodes #1-3 on the right side of the cord were positioned slightly ventral to the intermediolateral cell column (Figures 14, 15). The three electrode tips on the left side of the spinal cord were slightly deeper, within the dorsal part of the ventral horn. Acellular glial scars extended ventral from the tip sites of most of the electrode tracks. In some cases, the injury extended into the ventral funiculus, where the injury was manifested as spongy changes (Figure 15). The likely cause of this type of injury is discussed below. Also in cats Sp108, there were inflammatory foci around the tips of both pulsed electrodes (#1 and #2). The foci contained mostly small, round lymphocytes, and a few mononuclear cells. Neutrophils were absent. Neurons near the tips of the pulsed (Figure 16) and unpulsed (Figures 17,18) appeared normal.

Physiology

The effects of the prolonged stimulation on neuronal excitability was generally consistent with the histologic findings. Figure 19A shows a family of averaged responses evoked in the ventral roots from intraspinal microelectrode #1 of cat Sp106. Before the start of the first day (12 hours) of stimulation, the traces contain a single (primarily negative) response (*) with a latency slightly less than 1 ms, and with a threshold of approximately 23 μA. After the first and second 12-hour sessions of stimulation (80 μA at 20 Hz), the threshold and amplitude of the response was unchanged (Figures 19B and C). This is consistent with the histologic findings, in which most of the neurons adjacent to the site of the tips of (pulsed) microelectrode #1 and #6 appeared essentially normal. However, the threshold of the response is quite high, and probably does not reflect the effects of the stimulation on neurons that are very close to the microelectrodes, and at least one of which might have been damaged by the stimulation (Figure 5).

Figures 20A, B and C show the responses evoked from microelectrode #1 in cat Sp108. In this cat, electrodes #1 and #2 were pulsed for 12 hours at 100 μA and at 20 Hz. The evoked responses acquired before the first 12-hour session contain an early component (*) with a threshold of approximately 26 μA and a post-stimulus latency of approximately 1 ms. There is a second component (S) with a threshold of approximately 42 μA and a latency of approximately 1.5 ms. By the end of the first 12 hours of stimulation, the thresholds of both components had actually decreased slightly, and by the end of the second 12-hour session, the thresholds and amplitudes of both components were essentially as before the start of the first 12-hour session. Again, the rather high thresholds of these responses is an indication that they do not reflect stimulation-induced changes that may have occurred within a few μm of the electrode tips, and in particular any deleterious effect that may have accompanied the aggregation of lymphocytes around the pulsed tips sites (Figure 14 and 15). Rather, the responses probably are generated by the neurons slightly more distant from the electrode tips, and these appeared to be quite normal, in spite of the prolonged and intense stimulation (Figure 16).

DISCUSSION

In the present series, all 3 cats showed histological evidence that the microelectrode tips had penetrated into tissue that was ventral to their final depth of insertion. In cat Sp107, the interpretation of the histology is complicated by widespread injury due to a blunder during the implant surgery. However, the spinal cords of cats Sp106 and Sp108 also showed evidence of this problem. Glial scars extended ventrally from most of the final tip sites. In most cases, these elongated scars were not oriented precisely with the final electrode tracks. The scars were well healed and nearly acellular and there was little or no hemosiderin. These characteristics indicate that they had occurred early in the 30-day history of the implants. A frame-by-frame examination of the intraoperative video tapes confirmed that there had been transient displacement of the dorsal surfaces of the spinal cords during insertion of the electrode arrays. Figure 21C illustrates how the cord may have been momentarily compressed vertically, and expanded horizontally, at the end of the insertion stroke, so that tissue that normally would lie deep to the electrode sites would be raked up and across the electrode tips. Later, the cord would resume its normal configuration and the damaged tissue would return to its original location, deep to the electrode tips.

As illustrated in Figures 21A & B, three variables of the insertion process can be controlled. D1 is the distance between the lower end of the sliding cylinder and the orifice of the introducer instrument. This setting controls the amount by which the undersurface of the array will displace the surface of the cord at the end of the insertion stroke. If D1 is too large, the electrodes will not be inserted fully. If it is too small, the underside of the array will impact against the surface of the cord, and there will be risk of injury to the dorsal columns. Also, the cord will be displaced during the terminal phase of the insertion stroke. The second controllable variable is the "pre-dimpling" distance, D_{pre}, the amount by which the barrel of the introducer tube is allowed to displace the cord from its resting position, prior to implanting the array. The sacral spinal cord is suspended very loosely within the spinal canal and it has been our practice to help to stabilize it at the end of the introducer by pre-dimpling the cord by approximately 1 mm. The third controllable variable is the insertion velocity (Vi), which can be varied from a few centimeters per second to approximately 3 m/sec.

After examining the histologic sections from cats Sp106 and Sp107, we attempted to reduced the transient displacement of the cord during insertion of the array into cat Sp108 by setting D_{pre} to zero (no pre-dimpling of the cord surface), and also we reduced D1. In compensation for these changes, we increased the insertion velocity to approximately 2m/sec, so that the electrodes would be fully inserted. However, the intraoperative video still revealed displacement of the surface of the cord during the insertion stroke, and while the electrodes did insert fully (Figure 1C), the histologic examination revealed injury that is consistent with the cord having been momentarily compressed as illustrated in Figure 21C. Clearly, our strategy for inserting the electrodes into the sacral cord has not been optimal. In the next animal, D1 was adjusted so that at the end of the insertion stroke, the electrode superstructure's contoured underside will extend no further than the orifice of the introducer. With these settings, the array will not insert fully if the electrodes themselves cause any dimpling of the dura during insertion. If the electrodes do not insert fully, then the insertion velocity will be increased. We must then determine if the greater insertion velocity poses a risk of injury to parenchymal blood vessels. The histologic findings from these animals will be presented in the next report.

The Stimulus pulse amplitude and charge per phase used in these three animals was greater than in previous spinal cord series, and the pulsing rate was lower (20 Hz, vs 50 Hz). In cat Sp108, the tips of the two pulsed microelectrodes were surrounded by aggregates of lymphocytes. These electrodes had been pulsed at 100 μA (15 nC/phase) and at 20 Hz, continuously, for 12 hours on 2 consecutive days (the higher charge per phase used in any electrodes). The surface

areas of the electrodes is quite large (approximately 2,000 μm^2 geometric), and the charge density (750 $\mu C/cm^2$) was not excessive for anodically-biased activated iridium. In the spinal cord series, we have previously observed aggregates of lymphocytes around the tip of only one other electrode, which was pulsed for 24 hours at 50 μA and at 50 Hz. We have consistently observed these aggregates around pulsed microelectrodes in the cerebral cortex when the cats are sacrificed within 12 hours after the start of stimulation. However, the lymphocytes around the intracortical electrodes begin to disperse within approximately 48 hours, even when the stimulation is continued. We have attributed the absence of lymphocytes in the cat spinal cord to the fact that the stimulus regimens always spanned at least 36 hours. The presence of lymphocytes in cat Sp108 at 36 hours after the start of stimulation suggests that the aggregates may persist longer when the stimulus charge per phase is greater.

Figure 2. Sp106. A view of the dorsal surface of the aldehyde-fixed cat spinal cord, showing the electrode array superstructure, the tops of the 6 microelectrodes, and the stumps of their lead wires extending from the array in the rostral direction (arrowhead). This array was implanted within the S_2 region. The gradations on the rule are 1 millimeter.

Figure 3. Sp106. The track of pulsed electrode #1. The dorsal surface of the cord was not compressed by the array superstructure, which was originally enclosed within the connective tissue capsule (arrowheads). The site of the electrode tip (arrow) is slightly dorsal to its intended target of the intermediolateral cell column. Two darkened regions (*) are processing artifacts. Nissl stain. Bar = 500 µm.

Figure 4. Sp106. Higher magnification of the site of the tip (T) of pulsed electrode #1. Note the glial scar extending lateral and ventral to the electrode (*). The crescent-shaped entity adjacent to the tips site is a damaged neuron (arrowhead). Nissl stain. Bar = 50 µm.

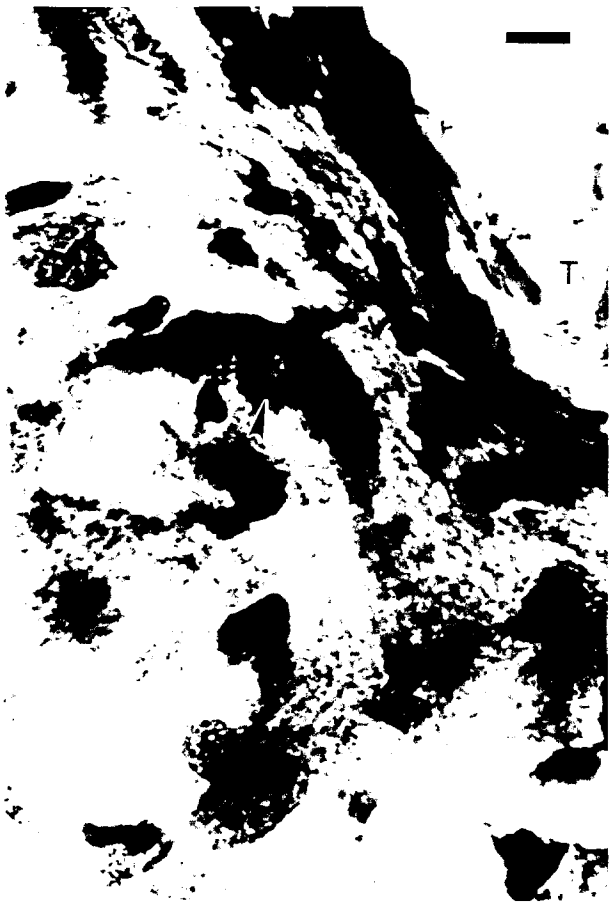

Figure 5. Sp106. Oil immersion micrograph of the tip site of pulsed electrode #1. Note the electrode capsule adjacent to the tip (T) and a hyperchromic, shrunken neuron (arrowhead) also shown in Figure 4. Nissl stain. Bar = 10 µm.

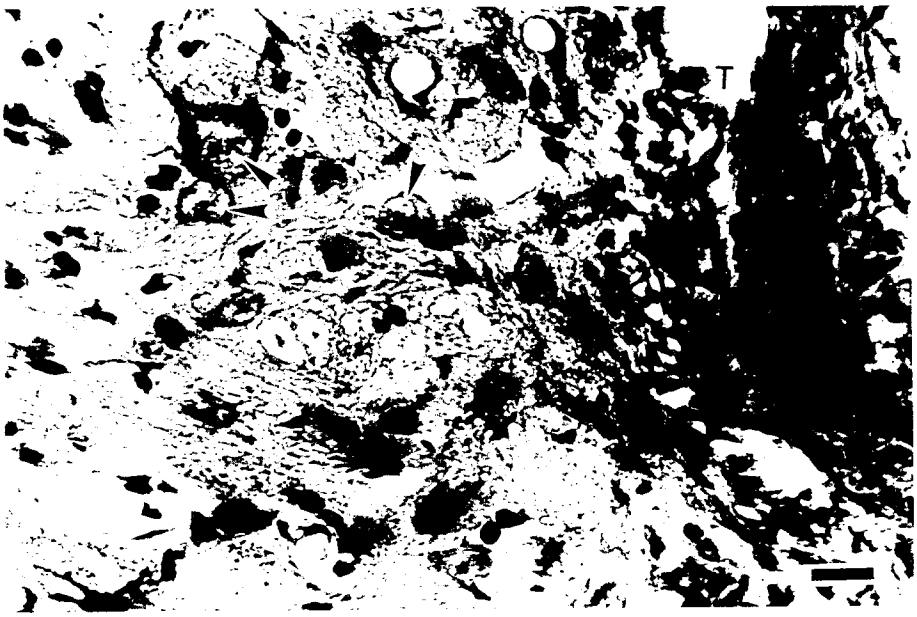

Figure 6. Sp106. A section through the site of the tip (T) of pulsed electrode #1. 8 µm lateral to the section shown in figure 4. Note several normal-appearing neurons (arrowheads) within 200 µm of the electrode tip. Nissl stain. Bar = 25 µm.

Figure 7. Sp106. The track and tip site of unpulsed electrode #2. The electrode tip (arrowhead) was located within the intermediolateral cell column. A pale, nearly acellular gliotic scar (*) ventral and medial to the tip site is also shown. Nissl stain. Bar = 500 µm.

Figure 8. Higher magnification of the field shown in Figure 7, showing the site of the tip (T) of unpulsed electrode #2. Note the healed glial scar (*) which probably was produced when the electrode overshot its target. Several normal-appearing neurons (arrowheads) lie within 200 µm of the tip, and lateral to the glial scar. Nissl stain. Bar = 50 µm.

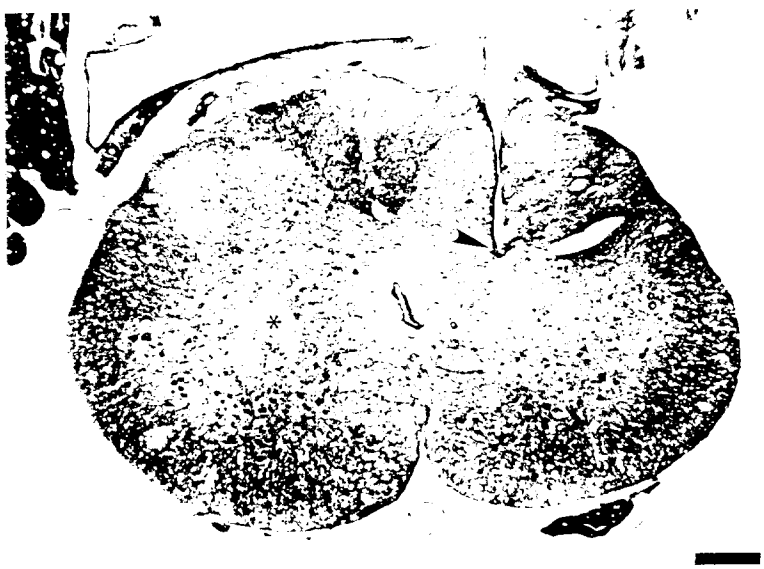

Figure 9. Sp106. The track and tip site (arrowhead) of unpulsed electrode #4, within the intermediolateral cell column. Note the gliotic scar (*) produced by another electrode in the opposite side of the cord, whose track is slightly rostral to this section. Nissl stain. Bar = 500 µm.

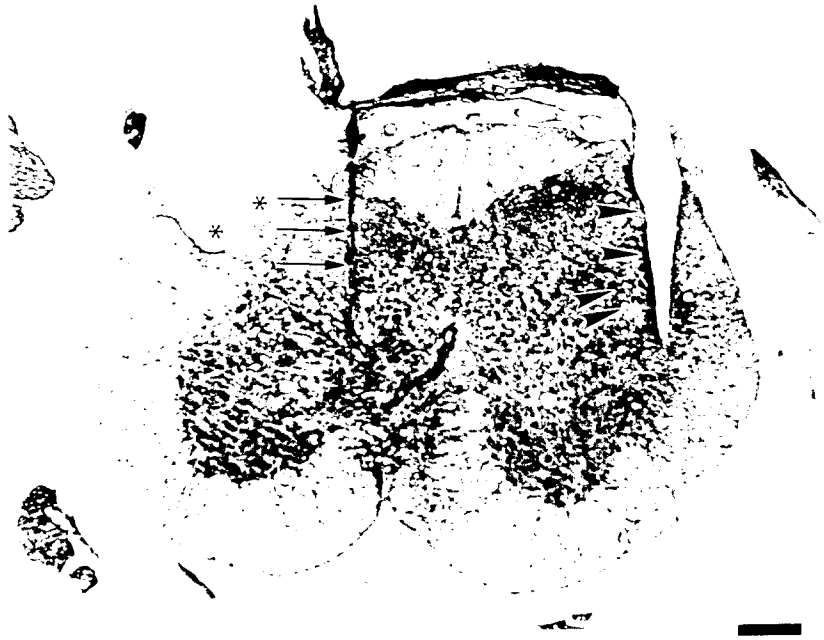

Figure 10. Sp107. A section through the track of unpulsed electrode #5 (right side of photograph - arrowheads; left side of cord in the animal), and through the sheath surrounding the capsule of electrode #2 (left side of photograph - arrows; right side of the cord in the animal). This array was reinserted manually, after it became partially dislodged during the implant surgery. Both electrode tracks and tip sites are surrounded by areas of extensive tissue injury. The double arrowheads indicates a region containing chromatolytic neurons shown in Figure 11. Note the compression (*) of the dorsal part of the cord produced by the array's superstructure. The connective tissue that had encapsulated the undersurface of the superstructure shifted during *post mortem* tissue handling and processing. Nissl stain. Bar = 500 µm.

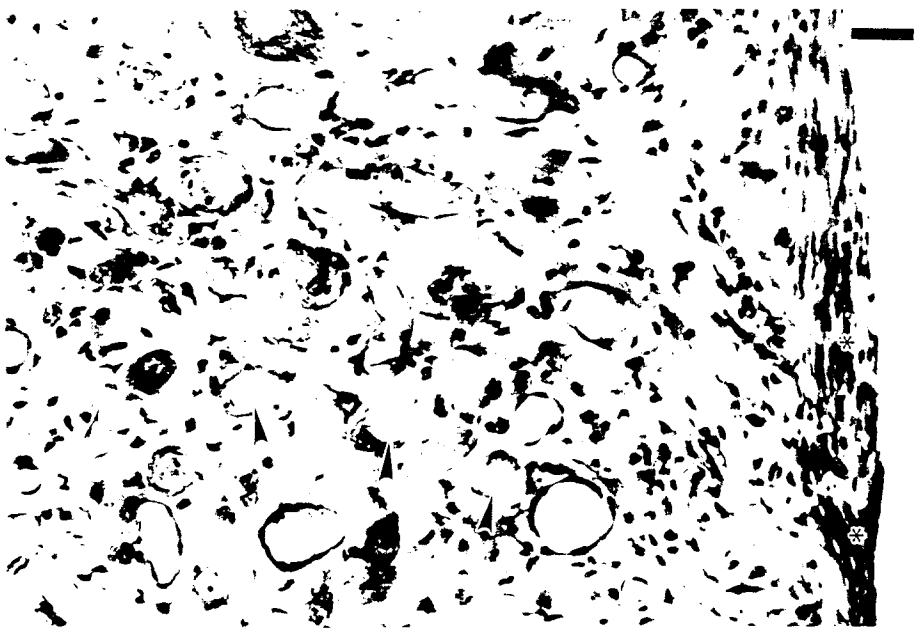

Figure 11. Sp107. Higher magnification of the area adjacent to the capsule (*) shown above in Figure 10 of unpulsed electrode #5. Several neurons are undergoing chromatolytic changes (arrowheads). Nissl stain. Bar = 50 µm.

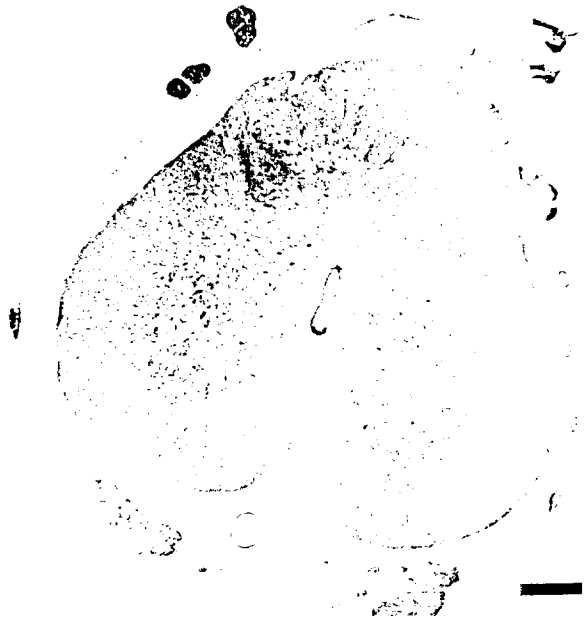

Figure 12. Sp107. A tissue section through S_3 of the spinal cord, and well caudal to the electrode array. The tissue was processed by Method B, as described in Methods, and sectioned at 6 µm. Nissl stain. Bar = 500 µm.

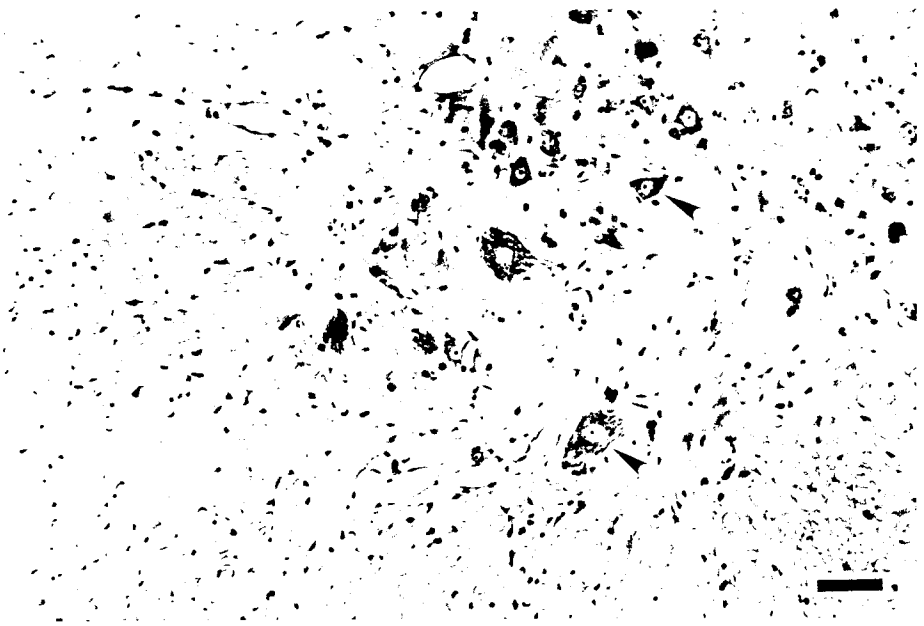

Figure 13. Sp107. Higher magnification of the ventral horn shown in Figure 12. Note the excellent definition of the neurons (arrowheads). Nissl stain. Bar = 50 µm.

Figure 14. Sp108. The track for pulsed electrode #1. There is an aggregation of lymphocytes surrounding the site of the electrode tip (arrowhead). Nissl stain. Bar = 500 µm.

Figure 15. Sp108. Higher magnification of the field in Figure 14, showing the site of the tip of pulsed electrode #1 and the aggregate of lymphocytes (arrowhead). A healed, nearly acellular gliotic scar is directed ventromedially from the tip site, toward the ventral funiculus (arrows). Within the lateral part of the ventral funiculus, on the opposite side of the cord, there is a gliotic scar and spongy changes (*) caused by another electrode whose final position was more dorsal, in the lateral ventral horn. Nissl stain. Bar = 200 µm.

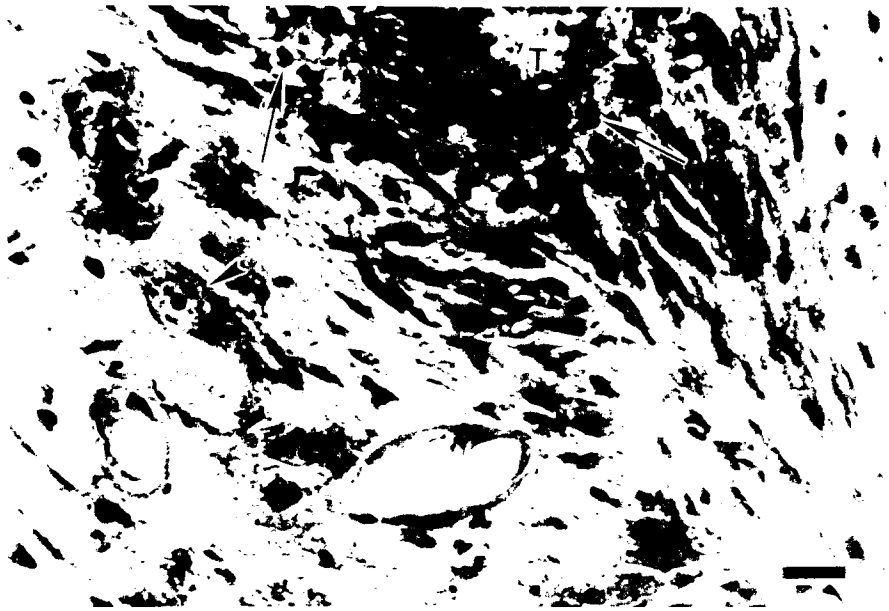

Figure 16. Sp 108. Higher magnification of the tip (T) of pulsed electrode #1 showing several small round leukocytes (arrows) and a normal-appearing neuron (arrowhead). Nissl stain. Bar = 25 µm.

Figure 17. Sp 108. The track and tip site from unpulsed electrode #3. The tip (arrowhead) is near the intermediolateral cell column. There are no lymphocytes surrounding the tip of this unpulsed electrode. Nissl stain. Bar = 500 µm.

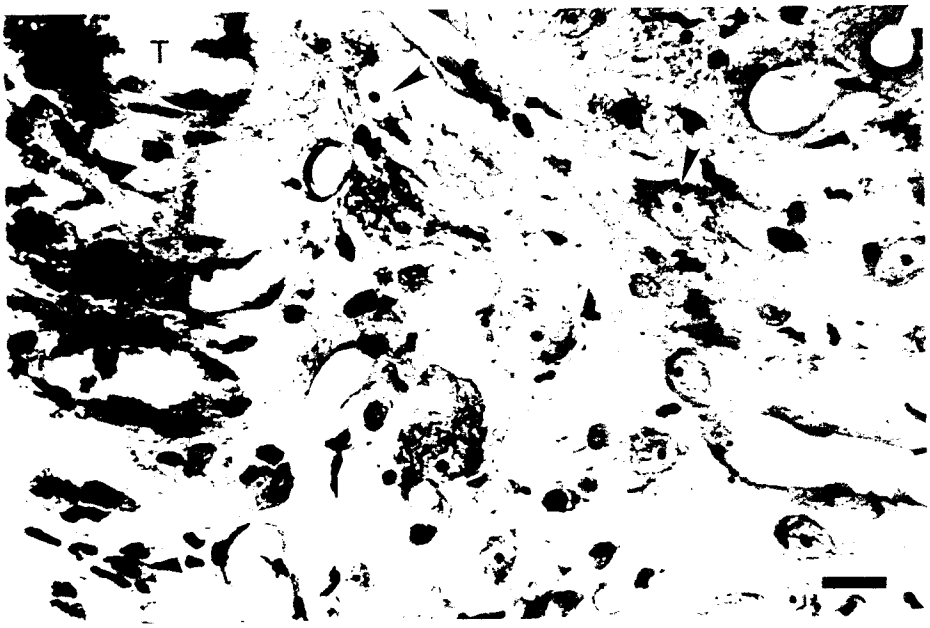

Figure 18. Sp108. Higher magnification of the tissue adjacent to the tip (T) of unpulsed electrode #3. Note the normal-appearing neurons (arrowheads) within 200 µm of the electrode tip, and the absence of lymphocytes. Nissl stain. Bar = 25 µm.

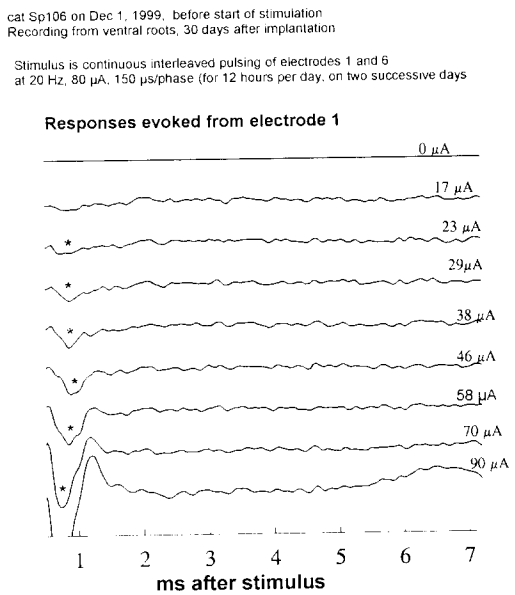

Figure 19A

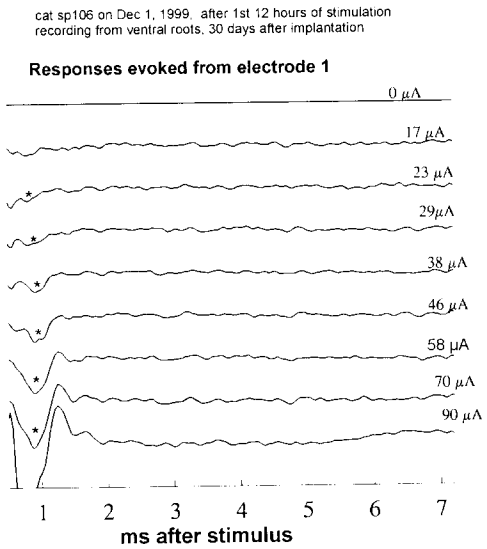

Figure 19B

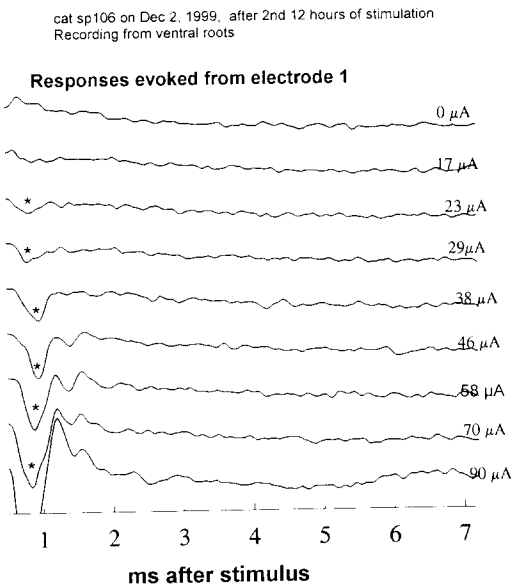

Figure 19C

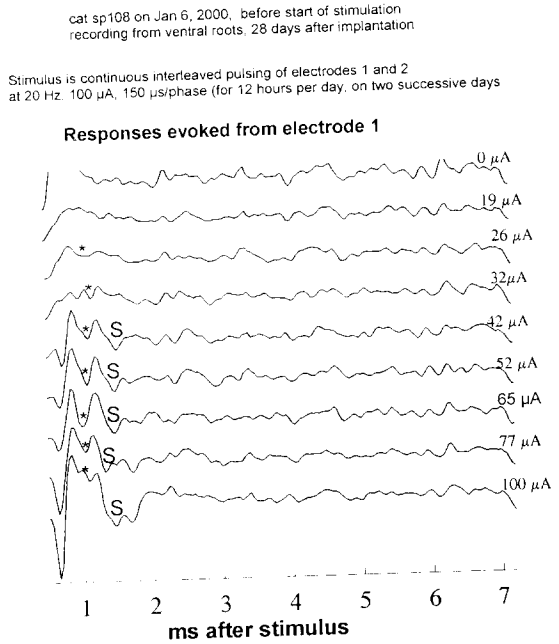

Figure 20A

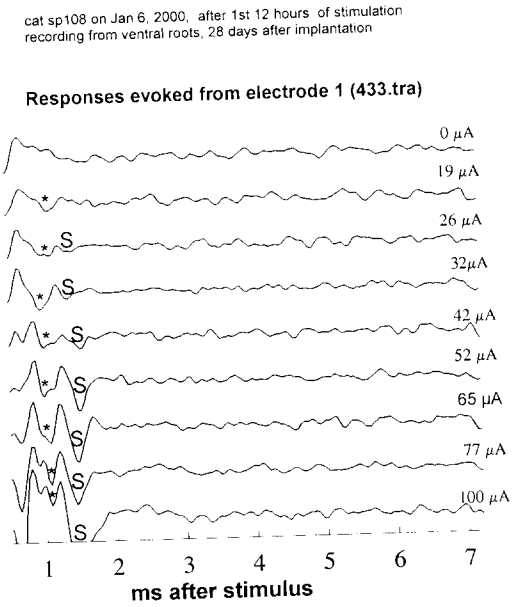

Figure 20B

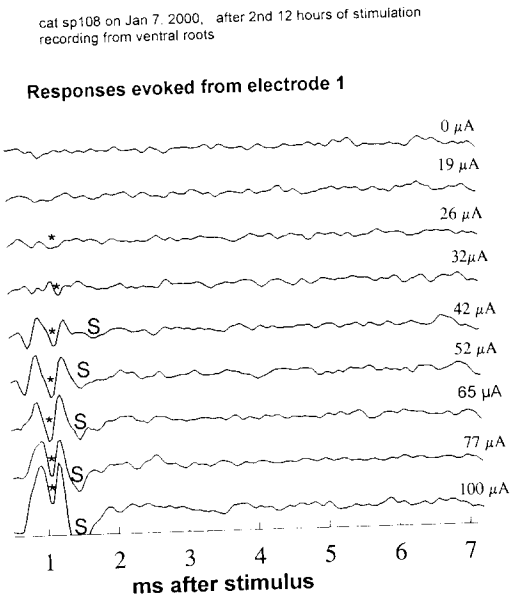

Figure 20C

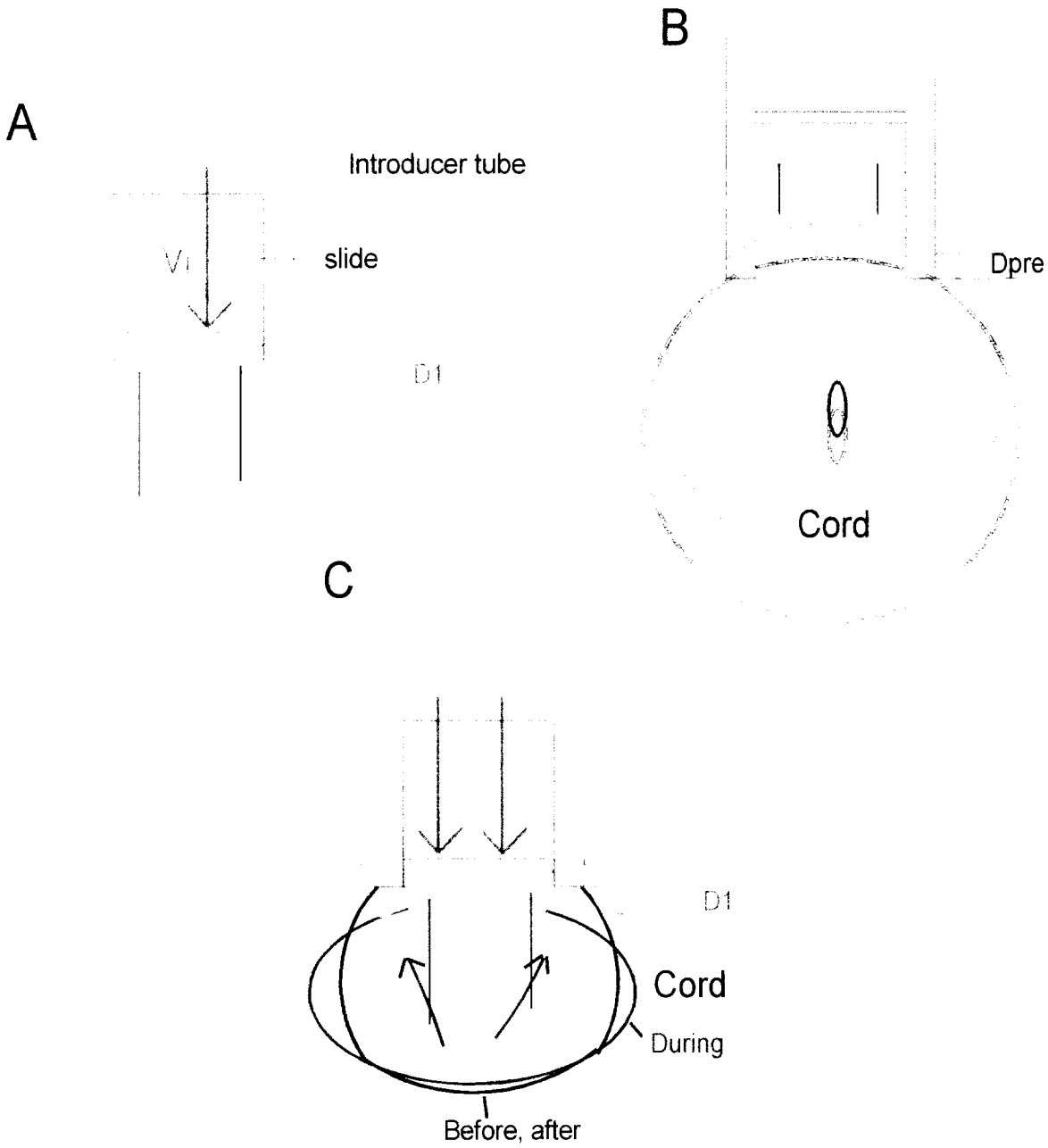
A
Introducer tube
V1
slide
D1
B
Dpre
Cord
C
D1
Cord
During
Before, after

Figure 21